Paleoenvironmental changes across the Mesozoic–Paleogene hyperthermal events

Tianchen He [a,b,*], David B. Kemp [c,**], Juan Li [d,**], Micha Ruhl [e,**]

[a] College of Oceanography, Hohai University, Nanjing 210024, China
[b] School of Earth and Environment, University of Leeds, Leeds LS2 9JT, UK
[c] State Key Laboratory of Biogeology and Environmental Geology and Hubei Key Laboratory of Critical Zone Evolution, School of Earth Sciences, China University of Geosciences, Wuhan 430074, China
[d] State Key Laboratory of Palaeobiology and Stratigraphy & Center for Excellence in Life and Paleoenvironment, Nanjing Institute of Geology and Palaeontology, Chinese Academy of Sciences, Nanjing 210008, China
[e] Department of Geology, Trinity College Dublin, The University of Dublin, Dublin 2, Ireland

ARTICLE INFO

ABSTRACT

Extreme climate warmth (hyperthermal) events through deep-time offer prescient insights into how the Earth may respond to present-day warming related to greenhouse gas emissions. This special issue deals with *Paleoenvironmental changes across the Mesozoic–Paleogene hyperthermal events* and comprises 25 interdisciplinary research articles. In this review paper, we summarise the contents of the special issue, placing it into a wider context, and demonstrate that Mesozoic–Paleogene hyperthermal events were among the most devastating and extreme climate modes in the geological record. Key findings are as follows: (1) Multi-proxy geochemical and sedimentological analyses reveal that widespread deoxygenation of oceans and megalakes was a common accompanying feature of most hyperthermals. (2) Evidence exists for complex linkages between volcanism, warm climate conditions, contemporary carbon cycles, aquatic biogeochemical cycles, wildfire activities, and climate-modulated hydrological and terrestrial weathering changes operating at seasonal, orbital and/or tectonic timescales. (3) Pronounced and rapid biological turnovers in the ocean during hyperthermals may have been linked to seawater acidification and shifts in nutrient availability, while promoting significant alterations in primary productivity, biological pump and ecosystem structures. Despite these advances, future interdisciplinary studies are needed to deliver a more comprehensive understanding of the nature and mechanism of complex environmental interactions within the Earth system, as well as the internal and external drivers that may have triggered hyperthermal events.

1. Introduction

Present-day global warming is likely occurring at an increasing rate, but predicting the consequences for marine and terrestrial environments and life remains a major challenge (Gruber et al., 2021; IPCC, 2022). There is a general consensus that current observations of extreme weather and biogeochemical changes are a precursor of future environmental and ecosystem changes at the decadal scale. However, predicting longer-term climatic and environmental responses to anthropogenic greenhouse gas forcing is difficult due to uncertainties in future emission rates, and uncertainties with respect to primary drivers and pathways in climate models (IPCC, 2022). Equally, the sensitivity of

the Earth system to climatic upheavals, and its ability to recover from them, is poorly known.

Geological records archive the potentially fatal consequences of sudden climate changes associated with global warming. Although driven by Earth's internal processes (e.g., the large-scale volcanism and release of CO_2 in particular), short-lived hyperthermal events in the geological past offer useful insights into how the Earth may respond to continued greenhouse gas release and warming at the present day (Foster et al., 2018; Hu et al., 2020) (Fig. 1). For instance, Song et al. (2021) recognize a potentially unifying feature between hyperthermal events in deep-time and present-day climate change. They propose that when certain relative temperature thresholds and rates of change are

breached, extreme deterioration of Earth's surface environment may occur triggering mass extinction. Probing into the different phases of deep-time hyperthermal episodes can not only inform us how the Earth system evolved as the climate warmed and cooled, but can also tell us how the Earth system responded to temperature changes of varying rates and magnitudes.

For this special issue, we have drawn together contributions focused on the major Mesozoic–Paleogene hyperthermals. The resulting collection helps elucidate the associated marine and terrestrial environmental changes and biological responses to these events over the last 250 Ma. These events include the Early–Middle Triassic hyperthermals (~250 Ma), the end-Triassic mass extinction event (ETME; ~201 Ma), the early Toarcian Oceanic Anoxic Event/Jenkyns Event (T-OAE; ~182 Ma), the Cretaceous Ocean Anoxic Events (OAEs; ~120 Ma to ~93 Ma), the Paleocene-Eocene Thermal Maximum (PETM; ~56 Ma) and other early Paleogene hyperthermals. The individual papers provide prescient insights into internal drivers, boundary conditions for climate shifts, Earth surface environmental effects and biogeochemical extremes across these major hyperthermal events. The interdisciplinary approaches used in the studies include stratigraphy, sedimentology, palaeontology, geochemistry and Earth system modelling.

In this Editorial Preface, we synthesize the findings of the contributing studies (Table 1), and in so doing we review current knowledge of the nature and consequences of the Mesozoic–Paleogene hyperthermals.

2. Large igneous province, hyperthermal conditions and carbon cycle

2.1. Carbon cycle perturbations

The Mesozoic–Paleogene hyperthermal events are commonly associated with a short-lived negative/positive carbon isotope excursions documented in marine and terrestrial sediments (e.g. ETME, T-OAE, OAE2, and PETM) (Hesselbo et al., 2002; Jenkyns, 2010; Kemp et al., 2005; Ruhl et al., 2011). These excursions reveal the impact of the events on the carbon cycle. Dong et al. (2022, this VSI) report new geochemical data from the Qumiba section in southern Tibet, which reveal a record of early Eocene paleo-climate conditions in the eastern Tethys ocean. Integration of multiple geochemical proxies suggest at least one early Eocene hyperthermal event (I1 or I2; ~53.6 Ma) was recorded in the Qumiba section, and was characterized by an abrupt negative carbon isotope excursion and enhanced chemical weathering. These new findings thus support warming-induced carbon cycle perturbation in the eastern Neo-Tethys Ocean.

Although the driver(s) for these carbon cycle perturbations are still debated, they are generally interpreted as linked to large scale, LIP-induced disruptions in the exogenic carbon cycle, for example through direct release of CO_2 from volcanoes, and/or via marine thermogenic methane release linked to magmatic intrusion of carbon-rich rocks or melting of methane clathrates (Capriolo et al., 2021; Hesselbo et al., 2002; Kemp et al., 2005; Ruhl et al., 2011). Yao et al. (2022a, this VSI) study a number of authigenic carbonates layers in a sequence of mid-Cretaceous inner shelf sedimentary rocks from the Qiangdong section,
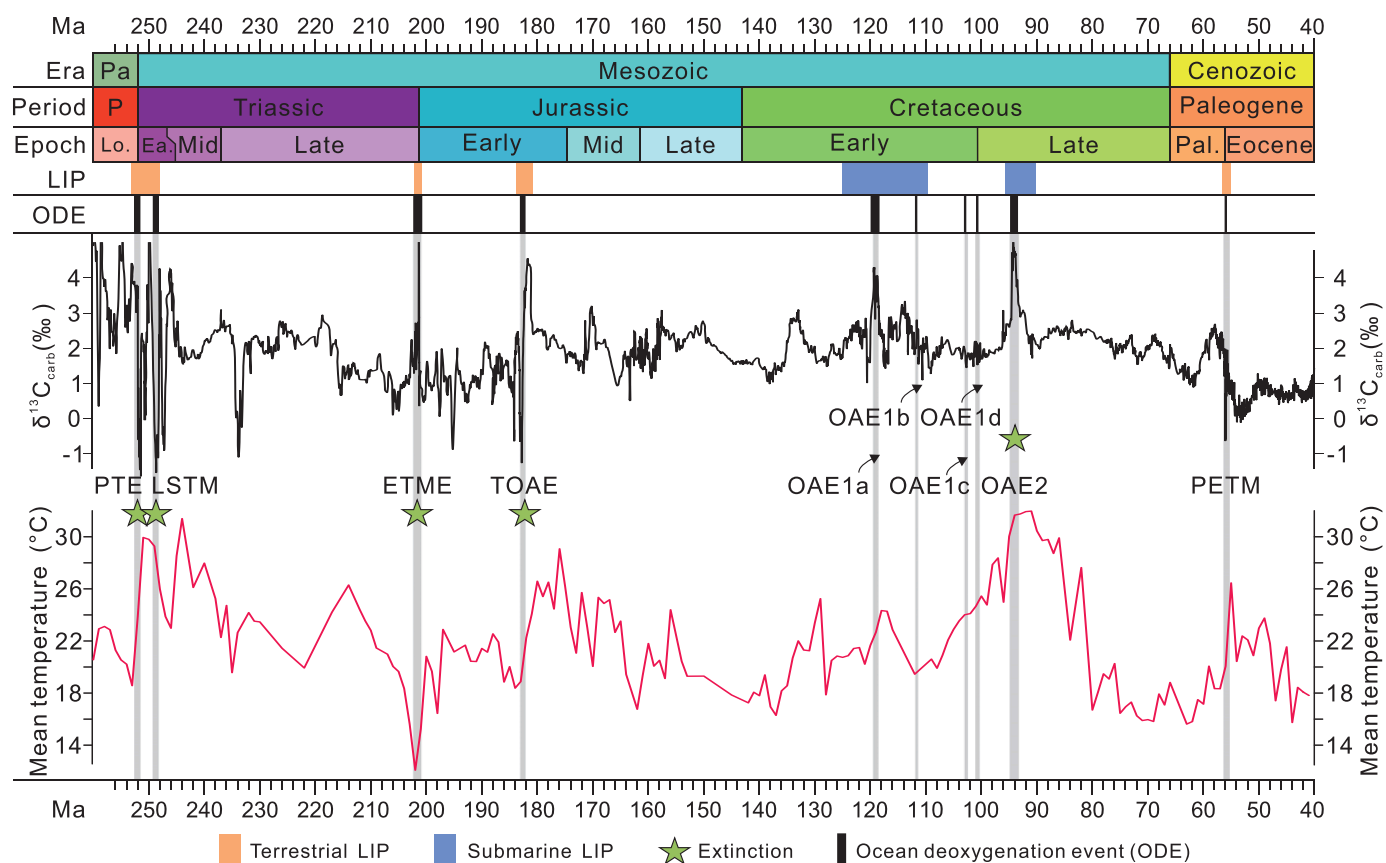

Fig. 1. Integrated records of climate conditions, carbon cycle perturbations and geological events during the Mesozoic–Paleogene hyperthermal events. The composite carbonate δ¹³C trend and the occurrences of marine anoxia, biotic crisis are presented from the Geologic Time Scale 2020 (Gradstein et al., 2020) and some new findings from this special issue. Long-term temperature record and the occurrences of Large igneous province (LIP) are based on Scotese et al. (2021) and Percival et al. (2018), respectively. PTE, Permian-Triassic extinction event; LSTM, Late Smithian Thermal Maximum; ETME, end-Triassic mass extinction event; TOAE, Toarcian Oceanic Anoxic Event; OAE, Oceanic Anoxic Event; PETM, Paleocene-Eocene Thermal Maximum.

Table 1

Summary of studied localities, events and paleoenvironment reconstructions in this special issue. ETM, Eocene Thermal Maximum; EECO, Early Eocene Climatic Optimum; MECO, Mid-Eocene Climatic Optimum; LOWE, Late Oligocene Warming Event; POE, Pre-Onset Excursion; METM, Middle Eocene Thermal Maximum; Pl/To, Pliensbachian–Toarcian boundary event.

	Study sites	Environment	Events/Interval	Age (Ma)	Topic	References
Paleogene hyperthermals						
1	Kutch, Cambay, Jaisalmer and Barmer basins, western India	restricted to open marine slope-basin margin	PETM, ETM2, ETM3, EECO, MECO, LOWE	56–23	glauconite formation and climatic warmth	Roy Choudhury et al., 2022
2	Zagros Folded Zone, SW Iran		POE, PETM, EECO, METM	57–42	storm-induced turbiditic events	Jiang et al., 2022
3	South Tibet, China	outer shelf	I1/I2	53.7–52.6	paleoclimate, weathering and marine redox	Dong et al., 2022
4	South Tibet, China	carbonate ramp	PETM	56	local controls on marine carbon cycle	Li et al., 2022
5	Tarim Basin, China	epicontinental sea	PETM	56	calcareous nannoplankton response	Wang et al., 2022
Cretaceous OAEs						
6	South Tibet, China	inner shelf	OAE1b, OAE2	112–94	hydrocarbon seepage activities	Yao et al., 2022a
7	Northwestern Tethys, Austria	hemipelagic ocean	OAE2	94	large igneous province and volcanism	Yao et al., 2022b
8	South Tibet, China	outer shelf	OAE1b, OAE1c	112, 102	orbital pacing and carbon cycle	Liu et al., 2022c
9	Yokonami Peninsula, Japan	deep-sea	OAE1a	120	enhanced hydrological cycle	Nakagawa et al., 2022
Toarcian Oceanic Anoxic Event / Jenkyns Event						
10	Hebrides Basin, UK	continental shelf	TOAE	183	marine redox and weathering changes	Chen et al., 2021
11	Inuyama area, central Japan	pelagic ocean	Pl/To, TOAE	185–183	marine redox conditions	Kemp et al., 2022a
12	NE Paris Basin, Luxembourg	continental shelf	TOAE	183	phytoplankton events	Ruebsam et al., 2022a
13	NE Paris Basin, Luxembourg	continental shelf	TOAE	183	biocalcification crisis	Ruebsam et al., 2022b
14	Sichuan Basin, China	lacustrine	TOAE	183	weathering and hydrological cycle	Liu et al., 2022b
15	Sichuan Basin, China	lacustrine	TOAE	183	lacustrine redox changes	Liu et al., 2022a
16	Yamaguchi Prefecture, Japan	pelagic ocean	Pl/To, TOAE	185–183	marine redox conditions	Chen et al., 2022
17	South Tibet, China	carbonate platform	Pl/To, TOAE	185–183	marine redox and weathering changes	Han et al., 2022
18	Ordos Basin, China	lacustrine	TOAE	183	lacustrine redox changes	Li et al., 2023
End-Triassic mass extinction						
19	Southern Italy	peritidal zone	ETME	202–200	marine redox conditions	He et al., 2022a
20	Bristol Channel and Larne basins, NW Europe	epicontinental sea	ETME	202–200	marine redox conditions	He et al., 2022b
21	Inuyama, Japan	pelagic ocean	ETME	202–200	biosiliceous productivity changes	Bôle et al., 2022
22	Lombardy Basin, Italy	carbonate platform	ETME	202–200	wildfire activity	Fox et al., 2022a
23	Cleveland and Bristol Channel basins, NW Europe	epicontinental sea	ETME	202–200	local controls on marine carbon cycle	Beith et al., 2023
Early–Middle Triassic hyperthermals						
24	Ordos Basin, China	lacustrine	Olenekian–Anisian	247	climate conditions and biotic recovery	Zhu et al., 2022
25	Chaohu Basin, China	carbonate platform	LSTM	250	magmatic degassing	Du et al., 2022

southern Tibet. Their field observations, thin section petrography, mineralogy, and stable isotope data indicate the occurrence of methane seepage across OAE 2. They propose that stimulated methanogenesis enabled a higher flux of benthic methane release, which promoted oxygen depletion in bottom-waters, thereby contributing to black shale deposition and providing a positive feedback conducive to organic matter preservation and burial during OAE 2.

A critical feature of the ETME in the European epicontinental sea is a set of negative excursions in the bulk organic carbon isotope record. These chemostratigraphic features are useful to help constrain and correlate the timing of extinction and changes to the global carbon cycle. The driving mechanisms remain somewhat elusive, though extensive volcanism from emplacement of the Central Atlantic Magmatic Province (CAMP) was likely a major factor. Magmatic intrusion into ^{13}C-depleted organic rich sediments may have been a key source of carbon (Davies et al., 2017). Other workers have suggested instead that mixing of ^{12}C-enriched carbon from fresh to brackish water in marginal seas could have caused the excursions (Fox et al., 2020).

A more detailed investigation of carbon cycle changes can be achieved through compound-specific isotope analysis (CSIA) of molecular fossils (biomarkers) that more directly record changes to the terrestrial and marine realms. Through CSIA, Beith et al. (2023, this VSI) find little evidence of changes to the isotopic composition of biomarkers derived from marine and terrestrial photosynthetic organisms (that would readily uptake increases in volcanic-driven ^{12}C) during shifts in the bulk organic carbon isotope record. These results suggest that local factors played an important role in the bulk organic carbon isotope record during the ETME.

Marine sedimentary archives have also demonstrated the modulation of medium- and long-period orbital eccentricity as a main feature of the Mesozoic and Cenozoic carbon cycle evolution (Huang et al., 2010; Ruhl et al., 2016; Storm et al., 2020). Liu et al., (2022c, this VSI) present high-resolution carbon isotope, magnetic susceptibility, total organic carbon data and spectra analysis from Nirang Section in Tibetan Himalaya. These new data for the first-time construct long-term secular variations in carbon cycle through the Albian, and demonstrate that cyclical changes in carbon cycling occurred during Albian warmth, modulated by seasonal variations in terrigenous input driven by the

orbital forcings.

2.2. Intensified volcanism

The Mesozoic–Paleogene hyperthermal events are all short-lived (~50 ka to ~2 Ma) (Adams et al., 2010; Foster et al., 2018; He et al., 2020; Hu et al., 2020; Luo et al., 2010; Newton et al., 2011; Yao et al., 2018), and universally linked to elevated greenhouse gas concentrations. A key postulated driver of these events has emerged in recent years, namely voluminous volcanism and consequent CO_2 release related to the emplacement of large igneous provinces (LIPs) (Fig. 1). Intensified degassing during either eruptive episodes or via magmatic intrusion in carbon-rich sediments would have allowed temperature to rise rapidly and transiently. Hence, tracing the impact of LIPs to temporally correlated hyperthermal events is clearly an important research direction.

Anomalous enrichments of Hg, and associated changes in Hg-isotopes in sedimentary rocks are promising indicators of volcanic activity, and have the potential to track the intensity and sources of LIP volcanism (e.g., Grasby et al., 2019; Percival et al., 2021). Yao et al. (2022b, this VSI) report the first Hg and Zn isotope records across OAE 2 from a hemipelagic section deposited in northwestern Tethys and located in present-day Austria. Prominent Hg concentration anomalies and a positive Δ^{199}Hg excursion indicate the occurrence of intense LIP volcanism on land at the onset of OAE 2 (also termed as "Cretaceous thermal maximum"). This activity resulted in an increased flux of isotopically light Zn sourced from the LIP to the oceans.

Environmental perturbations punctuated the recovery from the Permo-Triassic mass extinction, including two closely spaced events linked to elevated temperature occurred through the Smithian-Spathian transition: the Late Smithian Thermal Maximum and Smithian-Spathian boundary mass extinction(Sun et al., 2012; Zhang et al., 2019). Du et al. (2022, this VSI) investigate C—S isotope systematics through this key interval of the Early Triassic from deep water facies in South China. They identify coupled positive excursions in seawater δ^{13}C and δ^{34}S across both events. Their modelling results indicate an Early–Middle Smithian magmatic event, which released a large mass of carbon, as well as enhanced continental weathering, expanded oceanic anoxia. This anoxia may have ultimately triggered extinction. The environmental feedback mechanisms demonstrated in this study are likely compatible with other hyperthermal events driven by intense volcanism and greenhouse gas release.

3. Climate-modulated terrestrial weathering, hydrological changes and tropical storms

Hyperthermal conditions enhance chemical weathering, ultimately sequestering atmospheric CO_2 and simultaneously promoting delivery of nutrients and alkalinity to aquatic environments (e.g., Pogge von Strandmann, 2020). Increased erosion and perturbations to the hydrological cycle and weather systems on land are predicted consequences of warming. Previous work has revealed such impacts during hyperthermal events, notably at the PETM and T-OAE (Dunkley Jones et al., 2018; Pujalte et al., 2015; Han et al., 2018; Izumi et al., 2018). However, uncertainties remain regarding the precise sedimentological responses and expression of such changes, due at least in part to the sporadic preservation of geologic evidence for extreme weather.

3.1. Marine sedimentological changes

Dramatic environmental and climatic changes responses to global warming events can be faithfully archived in marine sedimentary record. However, our understanding of sedimentological responses to major hyperthermal events is far from complete. Enhanced erosion/chemical weathering and hydrological changes has been widely documented in both terrestrial and marine archives during the PETM (Dunkley Jones et al., 2018; Pogge Von Strandmann et al., 2021; Pujalte et al., 2015). However, the paleoenvironmental responses to the PETM and other early Paleogene hyperthermal events at regional to global scale, in particular from a sedimentological perspective, remain scarce in the eastern Tethys Ocean.

In the Tibetan Himalaya, new integrated sedimentological, biostratigraphic, and carbon isotope data are used to evaluate the impact of the PETM on a shallow-water carbonate platform from proximal southern parts of the northern Indian continental margin (Li et al., 2022, this VSI). The data show distinct sedimentary environmental changes associated with major biotic turnover at the PETM onset, notably a regression from open to restricted shallow-marine environments and intensified continental weathering. During the PETM recovery, sedimentation was dominated by renewed lagoonal deposits caused by sea-level fall. Jiang et al. (2022, this VSI) report the environmental consequences of early Paleogene climatic anomalies from deep-water turbidite-rich successions deposited along the Arabian continental margin in southwestern Iran. Integrated sedimentological, biostratigraphic, and stable-isotope analysis of the early Paleogene Pabdeh Formation show that an anomalous abundance of storm-induced proximal to distal turbidites occurred across intervals of global warmth. The data thus suggest a causal link between climate extremes and tropical storms during the early Paleogene hyperthermal events.

To the south of the Tethyan Himalaya, Roy Choudhury et al. (2022, this VSI) present high-resolution biostratigraphic and sedimentological data, combined with carbon isotope signatures, which reveal an exceptionally high abundance of glauconite corresponding to the early Paleogene hyperthermal events in the shallow marine basins of the western India margin. The authors propose that glauconite formed abundantly during hyperthermal events as a result of the convergence of favorable depositional conditions, including rapid transgression, reduced sedimentation rate, warm seawater conditions, enhanced chemical weathering, and enhanced supply of nutrients favoring dysoxic shallow shelves.

3.2. Terrestrial perturbations

Greenhouse effect and associated paleoenvironmental changes arising from hyperthermal events also exert an impact to the terrestrial system. For example, volcanism could have resulted in increased wildfires (Baker et al., 2017; Belcher et al., 2021), whilst enhanced terrestrial hydrological cycling as a result of heavy precipitation and storms would have boosted particulate detrital material and nutrient supply to riverine and lacustrine settings (Pogge von Strandmann et al., 2013; Xu et al., 2018, 2017).

Through analysis of polycyclic aromatic hydrocarbons (PAHs), which are compounds found in sediments that typically represent incomplete combustion of organic matter, Fox et al. (2022a, this VSI) find that periods of wildfire activity across the Triassic–Jurassic boundary coincide with marine extinctions. The work links marine and terrestrial ecosystem stress and finds evidence for widespread wildfire activity later in the sedimentary record that is comparatively less intense but represents a more global signature. Such finding highlights the importance of fire as an extinction mechanism.

Previous work has noted the likely significant expansion of paleolake systems in the mid-latitude Sichuan and Ordos basins of China during T-OAE warming (Jin et al., 2020; Xu et al., 2017). Li et al. (2023, this VSI) present petrographical and geochemical data from lower Toarcian black shales and mudstones from the Anya section in the northeastern Ordos Basin. The petrography, integrated with climate proxies and weathering indices, suggests that a warm-humid climate with sporadic semi humid-semiarid periods developed during the T-OAE and coincided with enhanced chemical weathering. On the other hand, Liu et al. (2022b, this VSI) discover that the Sichuan Basin has been spontaneously subject to the impacts of enhanced hydrological cycling, high-frequency storms and floods, and intensified continental

weathering across the T-OAE. Elevated temperature and a humid climate are believed to have been responsible for these extremes, which may have simultaneously promoted nutrient input to the basins.

Nakagawa et al. (2022, this VSI) report a palynological analysis of the Hauterivian to Cenomanian deep-sea chert succession from the Goshikinohama section in Yokonami Peninsula, Japan. Their results show a remarkable increase in terrestrial plant preservation in deep-sea chert linked to a massive plant discharge driven by an enhanced hydrological cycle during OAE 1a. They further propose that intensified storms and/or some degrees of sea-level change occurred due to the hyperthermal conditions across the OAE 1a.

Climate re-stabilization is a natural mechanism for environmental recovery following hyperthermal crises. The patterns and causes of Early–Middle Triassic biotic recovery on land following the end-Permian hyperthermal and mass extinction event remain puzzling. Zhu et al. (2022, this VSI) reveal that sedimentary environments in the northeastern Ordos Basin evolved from arid braided-eolian conditions during the Induan to semi-humid shallow lacustrine and meandering river systems during the Olenekian–Anisian. Combining evidence from carbonate $\delta^{13}C$ isotopes, geochemical proxies of weathering intensity and abundant fossil occurrences, the authors conclude that warm and semi-humid climate in the Olenekian–Anisian contributed to the biotic recovery following the Permo-Triassic mass extinction.

4. Biogeochemical extremes

4.1. Marine redox dynamics

In the modern oceans, rising global temperature would warm surface waters and potentially promote stratification, which may trigger a shift from oxygenated to suboxic or even anoxic conditions in bottom waters (Breitburg et al., 2018; Falkowski et al., 2011; Keeling et al., 2010; Oschlies, 2021). Determining the precise magnitude, spatiotemporal pattern and causes of redox changes during past OAEs thus has major implications for the prediction and understanding of present-day ocean deoxygenation. In addition, understanding marine redox changes during ancient hyperthermal events aids examination and understanding of the linked global biogeochemical cycles (e.g. the bioavailability of phosphorus and benthic methane production) (Beil et al., 2020; He et al., 2020; Jenkyns, 2010; Schobben et al., 2020).

One of the most pronounced hyperthermal events of the Mesozoic, the T-OAE, was associated with widespread deoxygenation. Evidence for deoxygenation and the associated deposition of organic-rich facies during this event been noted in many locations around the world (Kemp et al., 2022b), but redox conditions were highly variable between different basins, water depths and oceans. Notably, the global geographic spread of anoxic or suboxic conditions is not well constrained due to a paucity of open ocean and pelagic records.

Kemp et al. (2022a, this VSI) present redox-sensitive trace metal data through the deep-water chert succession exposed at Sakahogi, Japan, which reveal an extended interval of basinal anoxia that began prior to the Pliensbachian–Toarcian (Pl–To) boundary and continued to the end of the T-OAE. These findings suggest the Panthalassic Ocean may have been an important locus of deoxygenation and organic carbon burial during the early Toarcian, and that the spread of anoxia during the T-OAE was a globally distributed phenomenon. Chen et al. (2022, this VSI) also study the Sakahogi section, and present stable sulfur isotopes of reduced metal-bound sulfur $\delta^{34}S$ across the Pl-To and T-OAE from this site. They compared these data to those from a shallower site deposited on the margin of the Panthalassa Ocean (Sakuraguchi-dani section, Japan). Positive shifts in $\delta^{34}S$ across the Pl-To and T-OAE at Sakahogi were most likely controlled by elevated export production and/or preservation, while a positive shift in $\delta^{34}S$ on the shallow shelf Sakuraguchi-dani site were attributable mainly to elevated sedimentation rates. Hence, the discovery of the positive $\delta^{34}S$ excursion across the Pl-To at Sakahogi indicates a hitherto unrecognized perturbation to the deep-water sulfur cycle.

By contrast, on the more restricted northwest European shelf, Chen et al. (2021, this VSI) investigate a lower Toarcian succession on the Isle of Raasay, Scotland (Hebrides Basin). The identification of a negative carbon isotope excursion provides the first evidence of the T-OAE in Scotland. Element abundance data and sedimentological observations indicate elevated chemical weathering rates associated with enhanced hydrological cycling. Redox-sensitive trace element data demonstrate that oxic-suboxic bottom water conditions prevailed. This contrasts with evidence for pervasive anoxia/euxinia in nearby basins, and emphasizes how deoxygenation was spatially variable and likely dependent on water depth and basin hydrography.

Widely distributed biotic carbonate platforms were commonly modified by drowning or a shift to non-skeletal carbonates during T-OAE global warming along the whole southern margins of the Tethys. Enhanced terrigenous input and oxygen depletion are commonly believed to be the two main factors that are disadvantageous to benthic communities and shallow-water carbonate production in geological history, but their role in driving the early Toarcian carbonate platform crisis is uncertain (Krencker et al., 2020). Han et al. (2022, this VSI) present $CaCO_3$ content, and carbonate-hosted trace elements from the Tibetan shallow-water carbonate platform. The results show a coupled shift towards enhanced continental weathering and deoxygenation over the T-OAE interval, which suggests that the shallow ocean oxygen decline may have been driven by enhanced nutrient input and primary productivity beginning at Pl–To boundary. Enhanced continental weathering and deoxygenation could have played a significant role in the carbonate-platform crises in Tibet and elsewhere both prior to, and during, the T-OAE.

The Triassic–Jurassic boundary (T–J) was another pivotal time of severe environmental change which triggered mass extinction in the ocean (Ruhl et al., 2011; Song et al., 2021). Numerous lines of evidence indicate intensified marine anoxia prevailed the mid-depth water and some semi-restricted basins in the European epicontinental sea (Fox et al., 2022b; He et al., 2020; Jaraula et al., 2013; Jost et al., 2017). Nonetheless, the geographic spread of low oxygen conditions and the precise temporal and mechanistic links between deoxygenation and extinction remain elusive.

He et al. (2022a, this VSI) measure variations in iodine abundance through a late Triassic carbonate succession deposited in a peritidal setting in western Tethys. The results show a sharp drop in I/(Ca + Mg) coinciding with the local extinction level, which indicates that the shallow ocean underwent oxygen depletion and that this may have precipitated local benthic ecosystem collapse. Within the cotemporaneous marginal sea basins in Europe, recent paleontological work has shown a two-phase extinction pattern across the Triassic-Jurassic boundary (Wignall and Atkinson, 2020). It is unclear if both extinction phases were induced by marine anoxia, or potentially driven by other environmental stressors. He et al. (2022b, this VSI) investigate the marine redox dynamics across the ETME in two representative basins of the European epicontinental seaway. Their results confirm that toxic euxinic conditions developed across the T–J boundary in both basins, hence making this a likely kill mechanism for the second phase of local benthic animal extinction. By contrast, the initial extinction level in the latest Triassic (late Rhaetian) was likely not associated with intensified anoxia, but its timing is consistent with shallowing and/or ocean acidification (Fox et al., 2022b).

4.2. Lacustrine biogeochemistry

Various hypotheses and studies have been proposed for how hyperthermal conditions and biogeochemical feedbacks (e.g., redox changes and nutrient fluxes) interacted in the marine realm. However, the extreme climatic forcings associated with hyperthermals likely exerted an equivalent impact on land. In the context of the Mesozoic–Paleogene hyperthermal events, possible fluctuations in water-column redox,

nutrient supply and other biogeochemical dynamics in ancient lacustrine environment remain largely unknown.

During expansion of paleo-lakes in the Sichuan Basin and Ordos Basins in the T-OAE, elevated organic matter productivity and burial has been proposed as a negative feedback helping to sequester excess atmospheric pCO$_2$ from the Toarcian atmosphere (Xu et al., 2017). However, the mechanism(s) of organic matter accumulation in lacustrine environments, and the causal links this may have to the early Toarcian hyperthermal event is poorly understood. Li et al. (2023, this VSI) investigate the petrological and geochemical characteristics of the lower Jurassic lacustrine succession exposed in the northeast Ordos Basin of China. The authors demonstrate that enhanced seasonality in a monsoon regime coupled with changes in local redox conditions influenced the source, accumulation, and preservation of organic matter across the event.

Liu et al., (2022a, this VSI) determine the redox conditions in the lacustrine Sichuan Basin of SW China based on iron speciation and trace metal data in sediments across shallow to deep water settings. The results show that the water column in the Sichuan Basin experienced a significant shift to anoxic-ferruginous conditions during the T-OAE. The authors also demonstrate that the development of lacustrine anoxia was also likely accompanied by elevated benthic methane release and major shifts in nutrient such as available phosphorus, which possibly contributed to eutrophication and the production of toxic hydrogen sulfide due to enhanced sulfate reduction.

5. Biotic changes under hyperthermal conditions

Environmental disturbances occurred concomitant with the Mesozoic–Paleogene hyperthermal events, profoundly impacting marine ecosystems. Bôle et al. (2022, this VSI) report the first mm-scale deep-sea δ^{30}Si profile of radiolarian moulds across the ETME at the Katsuyama section, Japan. Two negative δ^{30}Si excursions are identified across the radiolarian extinction interval, which the authors argue reflects radiolarian productivity decreases. The authors further suggest that the first δ^{30}Si excursion event occurred on a less than kyr-scale, consistent with the equally short-lived faunal turnover on land.

It is widely acknowledged that calcareous nannofossils underwent prominent but short-lived turnover across the PETM (Bralower and Self-Trail, 2016). However, in the eastern Tethys records of calcareous nannofossils through the PETM are still scarce. Wang et al. (2022, this VSI) address this subject by investigating a continuous early Eocene succession in the Tarim Basin, northwestern China. Their results show a deteriorated preservation and extremely low abundance of nannofossils and carbonate content in sediments during the PETM, thus providing evidence for contemporaneous ocean acidification in the shallow water of Paratethys. The records also show a significant increase in the species *Neochiastozygus junctus* during the PETM, which is interpreted to indicate enhanced surface ocean productivity driven by nutrient surge linked to enhanced terrestrial weathering.

Whilst the response of marine invertebrates towards the T-OAE is well-documented, that of marine primary producers is poorly constrained and our current understanding is mainly inferred from changes in algae groups producing hard parts, such as calcareous nannoplankton and organic-walled dinoflagellates (Mattioli et al., 2009). Ruebsam et al. (2022a, this VSI) report a high-resolution study on molecular fossils and calcareous nannofossils across the T-OAE in the NE Paris Basin. They identify at least five distinct phytoplankton events across the T-OAE interval, each of which was characterized by a demise of red algae groups and shallow- and deep-dwelling calcareous nannoplankton, and a contemporaneous proliferation of opportunistic green algae groups. The data also show that phytoplankton events, particularly at the onset of the T-OAE, were accompanied by recurrent freshening of surface waters during warming periods, suggesting these were the primary ecological drivers. Ruebsam et al. (2022b, this VSI) further suggest that across the T-OAE in Europe there was a weakening of the biological

pump due to the biocalcification crisis. The mechanism proposed is that decreased calcareous nannoplankton populations in surfaces waters led to a reduction in mineral ballast, reducing and slowing the descent of sinking particulate organic matter. This mechanism is proposed to have been a key cause of the relatively low organic carbon burial rates observed in many European basins.

6. Synthesis

The twenty-five articles in this special issue represent a first-order observation of Earth surface environmental changes across the major Mesozoic–Paleogene hyperthermal events. They provide potentially useful analogues for the climatic and environmental responses to anthropogenic greenhouse gas forcing. Enhanced instability in carbon cycling, weathering, hydrological conditions and redox are identified. The temporal link that is often observed between these hyperthermals and volcanism and LIP emplacement emphasizes how large-scale carbon release may have induced these strong positive climate feedbacks and extremes, which had profound impacts on the natural environment and ecosystems, leading in some cases to large-scale mass extinction. Nevertheless, determining a common mechanism/driver for all the hyperthermal events required making simplifying assumptions regarding the extent, abruptness, rates and intensity of various climatic and environmental forcings, thus leading to a number of important caveats and uncertainties. Higher resolution analysis of paleoenvironmental changes and the application and correlation of different proxies is needed to weigh between all possible drivers and consequences, allowing distinction of processes operating on both long and short timescales. Continues efforts are required to constrain paleoenvironmental changes across a complete range of geographies, for example from shallow to deep ocean environments, in order to obtain a holistic picture. Examining possible links between environment-ecosystem changes in the context of fossil records and implementing Earth system modelling might also be useful in testing hypotheses and quantifying the tempo and magnitude of various environmental forcings during these major hyperthermals.

Declaration of Competing Interest

The authors declare that they have no known competing financial interests or personal relationships that could have appeared to influence the work reported in this paper.

Data availability

No data was used for the research described in the article.

References

Adams, D.D., Hurtgen, M.T., Sageman, B.B., 2010. Volcanic triggering of a biogeochemical cascade during Oceanic Anoxic Event 2. Nat. Geosci. 3, 201–204. https://doi.org/10.1038/ngeo743.

Baker, S.J., Hesselbo, S.P., Lenton, T.M., Duarte, L.V., Belcher, C.M., 2017. Charcoal evidence that rising atmospheric oxygen terminated early Jurassic Ocean anoxia. Nat. Commun. 8, 15018. https://doi.org/10.1038/ncomms15018.

Beil, S., Kuhnt, W., Holbourn, A., Scholz, F., Oxmann, J., Wallmann, K., Lorenzen, J., Aquit, M., Hassane Chellai, E., 2020. Cretaceous oceanic anoxic events prolonged by phosphorus cycle feedbacks. Clim. Past 16, 757–782. https://doi.org/10.5194/cp-16-757-2020.

Beith, S.J., Fox, C.P., Marshall, J.E.A., Whiteside, J.H., 2023. Compound-specific carbon isotope evidence that the initial carbon isotope excursion in the end-Triassic strata in northwest Tethys is not the product of CAMP magmatism. Glob. Planet. Chang. https://doi.org/10.1016/j.gloplacha.2023.104044, 104044.

Belcher, C.M., Mills, B.J.W., Vitali, R., Baker, S.J., Lenton, T.M., Watson, A.J., 2021. The rise of angiosperms strengthened fire feedbacks and improved the regulation of atmospheric oxygen. Nat. Commun. 12, 503. https://doi.org/10.1038/s41467-020-20772-2.

Bôle, M., Ushikubo, T., Hori, R.S., Baumgartner, P.O., Nakai, Y., Ikeda, M., 2022. Si isotope ratio of radiolaria across Triassic–Jurassic transition in a pelagic deep-sea bedded chert (Inuyama, Japan). Glob. Planet. Chang. 215, 103882 https://doi.org/10.1016/j.gloplacha.2022.103882.

Bralower, T.J., Self-Trail, J.M., 2016. Nannoplankton malformation during the Paleocene-Eocene thermal Maximum and its paleoecological and paleoceanographic significance. Paleoceanography 31, 1423–1439. https://doi.org/10.1002/2016PA002980.

Breitburg, D., Levin, L.A., Oschlies, A., Grégoire, M., Chavez, F.P., Conley, D.J., Garçon, V., Gilbert, D., Gutiérrez, D., Isensee, K., Jacinto, G.S., Limburg, K.E., Montes, I., Naqvi, S.W.A., Pitcher, G.C., Rabalais, N.N., Roman, M.R., Rose, K.A., Seibel, B.A., Telszewski, M., Yasuhara, M., Zhang, J., 2018. Declining oxygen in the global ocean and coastal waters. Science 1979, 359. https://doi.org/10.1126/science.aam7240.

Capriolo, M., Marzoli, A., Aradi, L.E., Ackerson, M.R., Bartoli, O., Callegaro, S., Dal Corso, J., Ernesto, M., Gouvêa Vasconcellos, E.M., de Min, A., Newton, R.J., Szabó, C., 2021. Massive methane fluxing from magma–sediment interaction in the end-Triassic Central Atlantic Magmatic Province. Nat. Commun. 12, 5534. https://doi.org/10.1038/s41467-021-25510-w.

Chen, W., Kemp, D.B., He, T., Huang, C., Jin, S., Xiong, Y., Newton, R.J., 2021. First record of the early Toarcian Oceanic Anoxic Event in the Hebrides Basin (UK) and implications for redox and weathering changes. Glob. Planet. Chang. 207, 103685 https://doi.org/10.1016/j.gloplacha.2021.103685.

Chen, W., Kemp, D.B., Newton, R.J., He, T., Huang, C., Cho, T., Izumi, K., 2022. Major sulfur cycle perturbations in the Panthalassic Ocean across the Pliensbachian-Toarcian boundary and the Toarcian Oceanic Anoxic Event. Glob. Planet. Chang. 215, 103884 https://doi.org/10.1016/j.gloplacha.2022.103884.

Davies, J.H.F.L., Marzoli, A., Bertrand, H., Youbi, N., Ernesto, M., Schaltegger, U., 2017. End-Triassic mass extinction started by intrusive CAMP activity. Nat. Commun. 8, 15596. https://doi.org/10.1038/ncomms15596.

Dong, Y., Convers, L.C., Jiang, S., Li, X., Zhu, P., Chen, H., Cui, Y., 2022. Reconstruction of the early Eocene paleoclimate and paleoenvironment of the southeastern Neo-Tethys Ocean. Glob. Planet. Chang. 215, 103875 https://doi.org/10.1016/j.gloplacha.2022.103875.

Du, Y., Song, Huyue, Algeo, T.J., Song, Haijun, Tian, L., Chu, D., Shi, W., Li, C., Tong, J., 2022. A massive magmatic degassing event drove the Late Smithian Thermal Maximum and Smithian–Spathian boundary mass extinction. Glob. Planet. Chang. 215, 103878 https://doi.org/10.1016/j.gloplacha.2022.103878.

Dunkley Jones, T., Manners, H.R., Hoggett, M., Turner, S.K., Westerhold, T., Leng, M.J., Pancost, R.D., Ridgwell, A., Alegret, L., Duller, R., Grimes, S.T., 2018. Dynamics of sediment flux to a bathyal continental margin section through the Paleocene-Eocene thermal Maximum. Clim. Past 14, 1035–1049. https://doi.org/10.5194/cp-14-1035-2018.

Falkowski, P.G., Algeo, T., Codispoti, L., Deutsch, C., Emerson, S., Hales, B., Huey, R.B., Jenkins, W.J., Kump, L.R., Levin, L.A., Lyons, T.W., Nelson, N.B., Schofield, O.S., Summons, R., Talley, L.D., Thomas, E., Whitney, F., Pilcher, C.B., 2011. Ocean deoxygenation: past, present, and future. EOS Trans. Am. Geophys. Union 92, 409–410. https://doi.org/10.1029/2011EO460001.

Foster, G.L., Hull, P., Lunt, D.J., Zachos, J.C., 2018. Placing our current "hyperthermal" in the context of rapid climate change in our geological past. Philos. Trans. R. Soc. A Math. Phys. Eng. Sci. https://doi.org/10.1098/rsta.2017.0086.

Fox, C.P., Cui, X., Whiteside, J.H., Olsen, P.E., Summons, R.E., Grice, K., 2020. Molecular and isotopic evidence reveals the end-Triassic carbon isotope excursion is not from massive exogenous light carbon. Proc. Natl. Acad. Sci. U. S. A. 117, 30171–30178. https://doi.org/10.1073/pnas.1917661117.

Fox, C.P., Holman, A.I., Rigo, M., Al Suwaidi, A., Grice, K., 2022a. Paleowildfire at the end-Triassic mass extinction: Smoke or fire? Glob. Planet. Chang. 218, 103974 https://doi.org/10.1016/j.gloplacha.2022.103974.

Fox, C.P., Whiteside, J.H., Olsen, P.E., Cui, X., Summons, R.E., Idiz, E., Grice, K., 2022b. Two-pronged kill mechanism at the end-Triassic mass extinction. Geology 50, 448–453. https://doi.org/10.1130/G49560.1.

Gradstein, F.M., Ogg, J.G., Schmitz, M.D., Ogg, G.M., 2020. Geologic Time Scale 2020. Elsevier. https://doi.org/10.1016/C2020-1-02369-3.

Grasby, S.E., Them, T.R., Chen, Z., Yin, R., Ardakani, O.H., 2019. Mercury as a proxy for volcanic emissions in the geologic record. Earth Sci. Rev. https://doi.org/10.1016/j.earscirev.2019.102880.

Gruber, N., Boyd, P.W., Frölicher, T.L., Vogt, M., 2021. Biogeochemical extremes and compound events in the ocean. Nature 600, 395–407. https://doi.org/10.1038/s41586-021-03981-7.

Han, Z., Hu, X., Kemp, D.B., Li, J., 2018. Carbonate-platform response to the Toarcian Oceanic Anoxic Event in the southern hemisphere: Implications for climatic change and biotic platform demise. Earth Planet. Sci. Lett. 489, 59–71. https://doi.org/10.1016/j.epsl.2018.02.017.

Han, Z., Hu, X., Hu, Z., Jenkins, H.C., Su, T., 2022. Geochemical evidence from the Kioto Carbonate Platform (Tibet) reveals enhanced terrigenous input and deoxygenation during the early Toarcian. Glob. Planet. Chang. 215, 103887 https://doi.org/10.1016/j.gloplacha.2022.103887.

He, T., Dal Corso, J., Newton, R.J., Wignall, P.B., Mills, B.J.W., Todaro, S., di Stefano, P., Turner, E.C., Jamieson, R.A., Randazzo, V., Rigo, M., Jones, R.E., Dunhill, A.M., 2020. An enormous sulfur isotope excursion indicates marine anoxia during the end-Triassic mass extinction. Sci. Adv. 6 https://doi.org/10.1126/sciadv.abb6704 eabb6704.

He, T., Newton, R.J., Wignall, P.B., Reid, S., Dal Corso, J., Takahashi, S., Wu, H., Todaro, S., di Stefano, P., Randazzo, V., Rigo, M., Dunhill, A.M., 2022a. Shallow ocean oxygen decline during the end-Triassic mass extinction. Glob. Planet. Chang. 210, 103770 https://doi.org/10.1016/j.gloplacha.2022.103770.

He, T., Wignall, P.B., Newton, R.J., Atkinson, J.W., Keeling, J.F.J., Xiong, Y., Poulton, S. W., 2022b. Extensive marine anoxia in the European epicontinental sea during the end-Triassic mass extinction. Glob. Planet. Chang. 210, 103771 https://doi.org/10.1016/j.gloplacha.2022.103771.

Hesselbo, S.P., Robinson, S.A., Surlyk, F., Piasecki, S., 2002. Terrestrial and marine extinction at the Triassic-Jurassic boundary synchronized with major carbon-cycle perturbation: a link to initiation of massive volcanism? Geology 30, 251. https://doi.org/10.1130/0091-7613(2002)030<0251:TAMEAT>2.0.CO;2.

Hu, X., Li, J., Han, Z., Li, Y.-X., 2020. Two types of hyperthermal events in the Mesozoic-Cenozoic: Environmental impacts, biotic effects, and driving mechanisms. Sci. China Earth Sci. 63, 1041–1058. https://doi.org/10.1007/s11430-019-9604-4.

Huang, C., Hesselbo, S.P., Hinnov, L., 2010. Astrochronology of the late Jurassic Kimmeridge Clay (Dorset, England) and implications for Earth system processes. Earth Planet. Sci. Lett. 289, 242–255. https://doi.org/10.1016/j.epsl.2009.11.013.

IPCC, 2022. Climate change 2022: Impacts, adaptation, and vulnerability. In: Pörtner, H.-O., Roberts, D.C., Tignor, M., Poloczanska, E.S., Mintenbeck, K., Alegría, A., Craig, M., Langsdorf, S., Löschke, S., Möller, V., Okem, A., Rama, B. (Eds.), Contribution of Working Group II to the Sixth Assessment Report of the Intergovernmental Panel on Climate Change. Cambridge University Press.

Izumi, K., Kemp, D.B., Itamiya, S., Inui, M., 2018. Sedimentary evidence for enhanced hydrological cycling in response to rapid carbon release during the early Toarcian oceanic anoxic event. Earth Planet. Sci. Lett. 481, 162–170. https://doi.org/10.1016/j.epsl.2017.10.030.

Jaraula, C.M.B., Grice, K., Twitchett, R.J., Böttcher, M.E., LeMetayer, P., Dastidar, A.G., Opazo, L.F., 2013. Elevated pCO2 leading to late Triassic extinction, persistent photic zone euxinia, and rising sea levels. Geology 41, 955–958. https://doi.org/10.1130/G34183.1.

Jenkyns, H.C., 2010. Geochemistry of oceanic anoxic events. Geochem. Geophys. Geosyst. 11, 1–30. https://doi.org/10.1029/2009GC002788.

Jiang, J., Hu, X., Garzanti, E., Li, J., BouDagher-Fadel, M.K., Sun, G., Xu, Y., 2022. Enhanced storm-induced turbiditic events during early Paleogene hyperthermals (Arabian continental margin, SW Iran). Glob. Planet. Chang. 214, 103832 https://doi.org/10.1016/j.gloplacha.2022.103832.

Jin, X., Shi, Z., Baranyi, V., Kemp, D.B., Han, Z., Luo, G., Hu, J., He, F., Chen, L., Preto, N., 2020. The Jenkyns Event (early Toarcian OAE) in the Ordos Basin, North China. Glob. Planet. Chang. 193, 103273 https://doi.org/10.1016/j.gloplacha.2020.103273.

Jost, A.B., Bachan, A., van de Schootbrugge, B., Lau, K.V., Weaver, K.L., Maher, K., Payne, J.L., 2017. Uranium isotope evidence for an expansion of marine anoxia during the end-Triassic extinction. Geochem. Geophys. Geosyst. 18, 3093–3108. https://doi.org/10.1002/2017GC006941.

Keeling, R.F., Körtzinger, A., Gruber, N., 2010. Ocean deoxygenation in a warming world. Annu. Rev. Mar. Sci. 2, 199–229. https://doi.org/10.1146/annurev.marine.010908.163855.

Kemp, D.B., Coe, A.L., Cohen, A.S., Schwark, L., 2005. Astronomical pacing of methane release in the early Jurassic period. Nature 437, 396–399. https://doi.org/10.1038/nature04037.

Kemp, D.B., Chen, W., Cho, T., Algeo, T.J., Shen, J., Ikeda, M., 2022a. Deep-ocean anoxia across the Pliensbachian-Toarcian boundary and the Toarcian Oceanic Anoxic Event in the Panthalassic Ocean. Glob. Planet. Chang. 212, 103782 https://doi.org/10.1016/j.gloplacha.2022.103782.

Kemp, D.B., Suan, G., Fantasia, A., Jin, S., Chen, W., 2022b. Global organic carbon burial during the Toarcian oceanic anoxic event: patterns and controls. Earth Sci. Rev. https://doi.org/10.1016/j.earscirev.2022.104086.

Krencker, F.N., Fantasia, A., Danisch, J., Martindale, R., Kabiri, L., el Ouali, M., Bodin, S., 2020. Two-phased collapse of the shallow-water carbonate factory during the late Pliensbachian–Toarcian driven by changing climate and enhanced continental weathering in the Northwestern Gondwana Margin. Earth Sci. Rev. https://doi.org/10.1016/j.earscirev.2020.103254.

Li, J., Hu, X., Garzanti, E., BouDagher-Fadel, M., 2022. Spatial heterogeneity in carbonate-platform environments and carbon isotope values across the Paleocene–Eocene thermal maximum (Tethys Himalaya, South Tibet). Glob. Planet. Chang. 214, 103853 https://doi.org/10.1016/j.gloplacha.2022.103853.

Li, B., Jin, X., Corso, J.D., Ogg, J.G., Lang, X., Baranyi, V., Preto, N., Franceschi, M., Qiao, P., Shi, Z., 2023. Complex pattern of environmental changes and organic matter preservation in the NE Ordos lacustrine depositional system (China) during the T-OAE (early Jurassic). Glob. Planet. Chang. 221, 104045 https://doi.org/10.1016/j.gloplacha.2023.104045.

Liu, J., Cao, J., He, T., Liang, F., Pu, J., Wang, Y., 2022a. Lacustrine redox variations in the Toarcian Sichuan Basin across the Jenkyns Event. Glob. Planet. Chang. 215, 103860 https://doi.org/10.1016/j.gloplacha.2022.103860.

Liu, R., Hu, G., Cao, J., Yang, R., Liao, Z., Hu, C., Pang, Q., Pang, P., 2022b. Enhanced hydrological cycling and continental weathering during the Jenkyns Event in a lake

system in the Sichuan Basin, China. Glob. Planet. Chang. 216, 103915 https://doi.org/10.1016/j.gloplacha.2022.103915.

Liu, X., Zhang, Y., Han, K., Batenburg, S.J., Guo, H., Ma, C., Yao, H., Fan, H., Wu, Q., Chen, X., 2022c. Chemo- and cyclostratigraphic records of the Albian from the Tethyan Himalaya of southern Tibet, China. Glob. Planet. Chang. 218, 103955 https://doi.org/10.1016/j.gloplacha.2022.103955.

Luo, G., Kump, L.R., Wang, Y., Tong, J., Arthur, M.A., Yang, H., Huang, J., Yin, H., Xie, S., 2010. Isotopic evidence for an anomalously low oceanic sulfate concentration following end-Permian mass extinction. Earth Planet. Sci. Lett. 300, 101–111. https://doi.org/10.1016/j.epsl.2010.09.041.

Mattioli, E., Pittet, B., Petitpierre, L., Mailliot, S., 2009. Dramatic decrease of pelagic carbonate production by nannoplankton across the early Toarcian anoxic event (T-OAE). Glob. Planet. Chang. 65, 134–145. https://doi.org/10.1016/j.gloplacha.2008.10.018.

Nakagawa, Y., Legrand, J., Bôle, M., Hori, R.S., Kuroda, J., Hasegawa, H., Ikeda, M., 2022. Terrestrial and marine organic matter evidence from a cretaceous deep-sea chert of Japan: Implications for enhanced hydrological cycle during the Aptian OAE 1a. Glob. Planet. Chang. 215, 103886 https://doi.org/10.1016/j.gloplacha.2022.103886.

Newton, R.J., Reeves, E.P., Kafousia, N., Wignall, P.B., Bottrell, S.H., Sha, J.-G., 2011. Low marine sulfate concentrations and the isolation of the European epicontinental sea during the early Jurassic. Geology 39, 7–10. https://doi.org/10.1130/G31326.1.

Oschlies, A., 2021. A committed fourfold increase in ocean oxygen loss. Nat. Commun. 12, 2307. https://doi.org/10.1038/s41467-021-22584-4.

Percival, L.M.E., Jenkyns, H.C., Mather, T.A., Dickson, A.J., Batenburg, S.J., Ruhl, M., Hesselbo, S.P., Barclay, R., Jarvis, I., Robinson, S.A., Woelders, L., 2018. Does large igneous province volcanism always perturb the mercury cycle? Comparing the records of Oceanic Anoxic event 2 and the end-cretaceous to other Mesozoic events. Am. J. Sci. 318, 799–860. https://doi.org/10.2475/08.2018.01.

Percival, L.M.E., Bergquist, B.A., Mather, T.A., Sanei, H., 2021. Sedimentary Mercury Enrichments as a Tracer of large Igneous Province Volcanism, pp. 247–262. https://doi.org/10.1002/9781119507444.ch11.

Pogge von Strandmann, P.A.E., Jenkyns, H.C., Woodfine, R.G., 2013. Lithium isotope evidence for enhanced weathering during Oceanic Anoxic Event 2. Nat. Geosci. 6, 668–672. https://doi.org/10.1038/ngeo1875.

Pogge von Strandmann, P.A.E., Kasemann, S.A., Wimpenny, J.B., 2020. Lithium and lithium isotopes in Earth's surface cycles. Elements 16, 253–258. https://doi.org/10.2138/gselements.16.4.253.

Pogge Von Strandmann, P.A.E., Jones, M.T., West, A.J., Murphy, M.J., Stokke, E.W., Tarbuck, G., Wilson, D.J., Pearce, C.R., Schmidt, D.N., 2021. Lithium isotope evidence for enhanced weathering and erosion during the paleocene-eocene thermal maximum. Sci. Adv. 7, 1–12. https://doi.org/10.1126/sciadv.abh4224.

Pujalte, V., Baceta, J.I., Schmitz, B., 2015. A massive input of coarse-grained siliciclastics in the Pyrenean Basin during the PETM: the missing ingredient in a coeval abrupt change in hydrological regime. Clim. Past 11, 1653–1672. https://doi.org/10.5194/cp-11-1653-2015.

Roy Choudhury, T., Khanolkar, S., Banerjee, S., 2022. Glauconite authigenesis during the warm climatic events of Paleogene: Case studies from shallow marine sections of Western India. Glob. Planet. Chang. 214, 103857 https://doi.org/10.1016/j.gloplacha.2022.103857.

Ruebsam, W., Mattioli, E., Schwark, L., 2022a. Molecular fossils and calcareous nannofossils reveal recurrent phytoplanktonic events in the early Toarcian. Glob. Planet. Chang. 212, 103812 https://doi.org/10.1016/j.gloplacha.2022.103812.

Ruebsam, W., Mattioli, E., Schwark, L., 2022b. Weakening of the biological pump induced by a biocalcification crisis during the early Toarcian Oceanic Anoxic Event. Glob. Planet. Chang. 217, 103954 https://doi.org/10.1016/j.gloplacha.2022.103954.

Ruhl, M., Bonis, N.R., Reichart, G.-J., Damsté, J.S.S., Kürschner, W.M., 2011. Atmospheric Carbon Injection Linked to End-Triassic Mass Extinction. Science 1979 (333), 430–434. https://doi.org/10.1126/science.1204255.

Ruhl, M., Hesselbo, S.P., Hinnov, L., Jenkyns, H.C., Xu, W., Riding, J.B., Storm, M., Minisini, D., Ullmann, C.V., Leng, M.J., 2016. Astronomical constraints on the duration of the early Jurassic Pliensbachian Stage and global climatic fluctuations. Earth Planet. Sci. Lett. 455, 149–165. https://doi.org/10.1016/j.epsl.2016.08.038.

Schobben, M., Foster, W.J., Sleveland, A.R.N., Zuchuat, V., Svensen, H.H., Planke, S., Bond, D.P.G., Marcelis, F., Newton, R.J., Wignall, P.B., Poulton, S.W., 2020. A nutrient control on marine anoxia during the end-Permian mass extinction. Nat. Geosci. 13, 640–646. https://doi.org/10.1038/s41561-020-0622-1.

Scotese, C.R., Song, H., Mills, B.J.W., van der Meer, D.G., 2021. Phanerozoic paleotemperatures: the earth's changing climate during the last 540 million years. Earth Sci. Rev. 215, 103503 https://doi.org/10.1016/j.earscirev.2021.103503.

Song, Haijun, Kemp, D.B., Tian, L., Chu, D., Song, Huyue, Dai, X., 2021. Thresholds of temperature change for mass extinctions. Nat. Commun. 12, 4694. https://doi.org/10.1038/s41467-021-25019-2.

Storm, M.S., Hesselbo, S.P., Jenkyns, H.C., Ruhl, M., Ullmann, C.V., Xu, W., Leng, M.J., Riding, J.B., Gorbanenko, O., 2020. Orbital pacing and secular evolution of the early Jurassic carbon cycle. Proc. Natl. Acad. Sci. 117, 3974–3982. https://doi.org/10.1073/pnas.1912094117.

Sun, Y., Joachimski, M.M., Wignall, P.B., Yan, C., Chen, Y., Jiang, H., Wang, L., Lai, X., 2012. Lethally Hot Temperatures during the early Triassic Greenhouse. Science 1979 (338), 366–370. https://doi.org/10.1126/science.1224126.

Wang, Yasu, Cui, Y., Su, H., Jiang, J., Wang, Yang, Yang, Z., Hu, X., Jiang, S., 2022. Response of calcareous nannoplankton to the Paleocene–Eocene Thermal Maximum in the Parathethys Seaway (Tarim Basin, West China). Glob. Planet. Chang. 217, 103918 https://doi.org/10.1016/j.gloplacha.2022.103918.

Wignall, P.B., Atkinson, J.W., 2020. A two-phase end-Triassic mass extinction. Earth Sci. Rev. 208, 103282 https://doi.org/10.1016/j.earscirev.2020.103282.

Xu, W., Ruhl, M., Jenkyns, H.C., Hesselbo, S.P., Riding, J.B., Selby, D., Naafs, B.D.A., Weijers, J.W.H., Pancost, R.D., Tegelaar, E.W., Idiz, E.F., 2017. Carbon sequestration in an expanded lake system during the Toarcian oceanic anoxic event. Nat. Geosci. 10, 129–134. https://doi.org/10.1038/ngeo2871.

Xu, W., Ruhl, M., Jenkyns, H.C., Leng, M.J., Huggett, J.M., Minisini, D., Ullmann, C.V., Riding, J.B., Weijers, J.W.H., Storm, M.S., Percival, L.M.E., Tosca, N.J., Idiz, E.F., Tegelaar, E.W., Hesselbo, S.P., 2018. Evolution of the Toarcian (early Jurassic) carbon-cycle and global climatic controls on local sedimentary processes (Cardigan Bay Basin, UK). Earth Planet. Sci. Lett. 484, 396–411. https://doi.org/10.1016/j.epsl.2017.12.037.

Yao, W., Paytan, A., Wortmann, U.G., 2018. Large-scale ocean deoxygenation during the paleocene-eocene thermal maximum. Science 1979 (361), 804–806. https://doi.org/10.1126/science.aar8658.

Yao, H., Chen, X., Brunner, B., Birgel, D., Lu, Y., Guo, H., Wang, C., Peckmann, J., 2022a. Hydrocarbon seepage in the mid-cretaceous greenhouse world: a new perspective from southern Tibet. Glob. Planet. Chang. 208, 103683 https://doi.org/10.1016/j.gloplacha.2021.103683.

Yao, H., Chen, X., Wagreich, M., Grasby, S.E., Liu, S.-A., Yin, R., Tostevin, R., Lv, Y., Gu, X., Liu, X., Wang, C., 2022b. Isotopic evidence for changes in the mercury and zinc cycles during Oceanic Anoxic Event 2 in the northwestern Tethys, Austria. Glob. Planet. Chang. 215, 103881 https://doi.org/10.1016/j.gloplacha.2022.103881.

Zhang, L., Orchard, M.J., Brayard, A., Algeo, T.J., Zhao, L., Chen, Z.Q., Lyu, Z., 2019. The Smithian/Spathian boundary (late early Triassic): a review of ammonoid, conodont, and carbon-isotopic criteria. Earth Sci. Rev. https://doi.org/10.1016/j.earscirev.2019.02.014.

Zhu, Z., Liu, Y., Kuang, H., Newell, A.J., Peng, N., Cui, M., Benton, M.J., 2022. Improving paleoenvironment in North China aided Triassic biotic recovery on land following the end-Permian mass extinction. Glob. Planet. Chang. 216, 103914 https://doi.org/10.1016/j.gloplacha.2022.103914.